Absorptive Frequency-Selective Transmission Structure With Square-Loop Hybrid Resonator

Hao Huang, *Student Member, IEEE*, and Zhongxiang Shen, *Fellow, IEEE*

***Abstract*—A novel design of an absorptive frequency-selective transmission structure (AFST) is proposed. This structure is based on the design of a frequency-dependent lossy layer with square-loop hybrid resonator (SLHR). The parallel resonance provided by the hybrid resonator is utilized to bypass the lossy path and improve the insertion loss. Meanwhile, the series resonance of the hybrid resonator is used for expanding the upper absorption bandwidth. Furthermore, the absorption for out-of-band frequencies is achieved by using four metallic strips with lumped resistors, which are connected with the SLHR. The quantity of lumped elements required in a unit cell can be reduced by at least 50% compared to previous structures. The design guidelines are explained with the aid of an equivalent circuit model. Both simulation and experiment results are presented to demonstrate the performance of our AFST. It is shown that an insertion loss of 0.29 dB at 6.1 GHz and a 112.4% 10 dB reflection reduction bandwidth are obtained under the normal incidence.**

***Index Terms*—Absorptive frequency-selective structure, equivalent circuit model, frequency-selective rasorber (FSR).**

I. Introduction

FREQUENCY-SELECTIVE structures are important in many civil and defense communication systems for their spatial filtering characteristics [1]. In many applications, it is highly desirable that a frequency-selective structure can only transmit the signals within a required frequency range. Moreover, the signals outside the frequency range are absorbed with this structure. To achieve this purpose, a new type of structure named absorptive frequency-selective transmission structure (AFST) [2] or frequency-selective rasorber [3] has been introduced.

In general, this structure has unique features with an absorption–transmission–absorption response. In this case, the in-band signal is transmitted through the radome with low insertion loss. Meanwhile, the out-of-band signal is substantially absorbed. Two different methods have been proposed in the literature to obtain this type of frequency response. One way is based on constructing absorption and transmission paths separately with lossless and lossy resonators in a three-dimensional (3-D) unit cell [2]–[5]. These 3-D structures have an advantage of stable performance at the oblique incidence. The other way is cascading a lossy layer above a lossless bandpass frequency selective surface (FSS). Especially for the second configuration, the main limitation is its insertion loss, with a lossy layer inevitably inserted in the propagation path.

In the past, the transmission band and absorption band were chosen at two separate bands [6]–[8]. Under this situation, the performance of transmission is not affected by the lossy components. However, this configuration can only achieve one-sided absorption (lower or upper absorption band). After that, several techniques aiming at achieving a transmission window within an absorption band have been proposed. To improve the insertion loss, the intuitive way is to bypass the lossy components at the transmission band. This idea was implemented in [9]. However, this rasorber is rather complicated, which consumes several lumped elements with different values. Another way is to cut off the current flow on the lossy path. This technique was realized by loading lumped *LC* resonators in [10], or using meander line and parallel gap sections to mimic parallel lumped *LC* components in [11], and utilizing a short-circuited quarter-wavelength transformer to choke current flow through resistors in [12]. Meanwhile, the main disadvantage for the designs in [11] and [12] is that they only have absorption band below a transmission window. Apart from that, Xiu *et al.* [13] realized a dual-polarized performance by rotationally duplicating the unit cell in [12]. Therefore, it is still a challenge for AFST to minimize the insertion loss and maximize the absorption bandwidth.

In this letter, a new structure is presented to obtain a transmission window with low insertion loss and a wide absorption band at the same time. This is achieved by utilizing a square-loop hybrid resonator (SLHR). Based on its equivalent circuit model, a detailed analysis is given to explain the existence of the parallel and series resonances of SLHR and the techniques to utilize these resonances in the design of an AFST.

II. Design and Analysis of Structure

The proposed unit cell of our AFST is illustrated in Fig. 1(a). It consists of two layers of printed circuit boards, which are separated by an air spacer. It is seen that the first layer is an SLHR connected by four metallic strips. Resistors are soldered between these metallic strips to provide the desired absorption at certain frequencies. The second layer is a bandpass FSS. From the equivalent circuit model in Fig. 2(a), we may find that the backed bandpass FSS plays a very importance role in the impedance matching of absorption layer with free space. To facilitate the analysis, the impedances of the first and the second layers are represented by Z_{F1} and Z_{F2}, respectively.

Manuscript received September 12, 2017; revised October 23, 2017; accepted October 27, 2017. Date of publication November 2, 2017; date of current version December 11, 2017. *(Corresponding Author: Hao Huang.)*

The authors are with the School of Electrical and Electronic Engineering, Nanyang Technological University, Singapore 639798 (e-mail: hhuang019@e.ntu.edu.sg; ezxshen@ntu.edu.sg).

Color versions of one or more of the figures in this letter are available online at http://ieeexplore.ieee.org.

Digital Object Identifier 10.1109/LAWP.2017.2769093

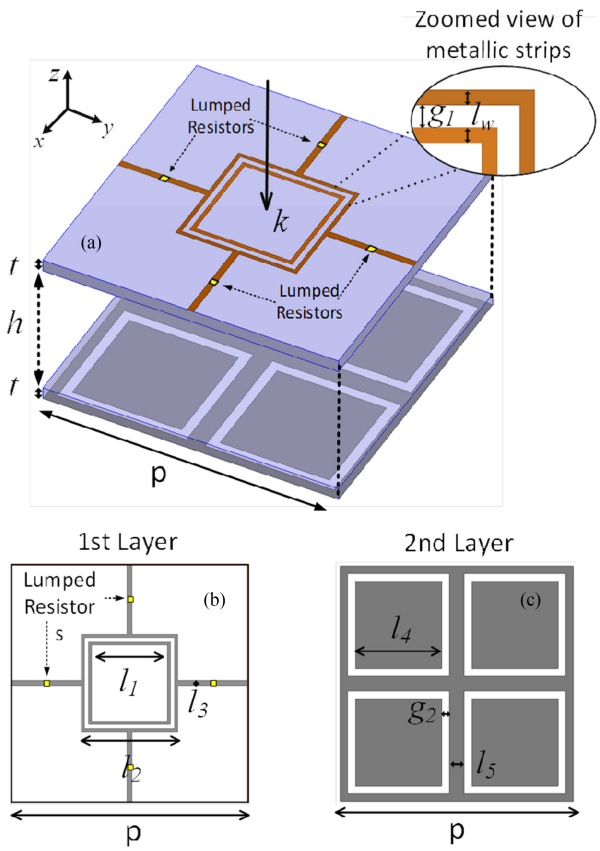

Fig. 1. (a) Unit cell structure of proposed AFST. (b) SLHR and resistor strips on the first layer. (c) Bandpass FSS at the second layer. (Dimensions: $p = 24$ mm, $t = 1$ mm, $h = 11$ mm, $l_1 = 7.3$ mm, $l_2 = 9.8$ mm, $l_3 = 0.5$ mm, $l_4 = 8.88$ mm, $l_5 = 1.52$ mm, $l_w = 0.5$ mm, $g_1 = 0.25$ mm, $g_2 = 0.8$ mm, $\varepsilon_r = 3$, $R_a = 294\,\Omega$.)

The impedance looking into the spacing between the substrates and the bandpass FSS is represented by Z_{in}. It is clear to see from Fig. 2(b) that the impedance of lossy path Z_{F1} matches well with the characteristic impedance of free space near the frequencies of f_{r0} and f_{r2}. To achieve a good absorption, the impedance Z_{in} has to satisfy $Z_{\text{in}} = \infty$, which means the current can only flow through the lossy path with substantial absorption. To simplify this equation, we may ignore the effects of the substrate due to its small electrical length, and the impedance Z_{F2} is expressed as

$$Z_{F2} = \frac{j\omega L_f}{1 - \omega^2 L_f C_f}. \tag{1}$$

The ABCD matrix of the two-port network for the air spacer and bandpass FSS is written as

$$\begin{bmatrix} A & B \\ C & D \end{bmatrix} = \begin{bmatrix} \cos\theta_2 & jZ_2 \sin\theta_2 \\ jY_2 \sin\theta_2 & \cos\theta_2 \end{bmatrix} \begin{bmatrix} 1 & 0 \\ Y_{F2} & 1 \end{bmatrix}. \tag{2}$$

This ABCD matrix can be transformed into Z matrix. Since $Z_{\text{in}} = \text{Z}_{11}$, we may set $1/\text{Z}_{11} = 0$ to obtain the desired two absorption frequencies, which can be solved from

$$\tan(\theta_2) = Z_2 \left(\frac{1}{2\pi f L_f} - 2\pi f C_f \right) \tag{3}$$

where $\theta_2 = 2\pi f h/c$, c is the speed of light and h is the spacing between two substrates. The two solutions of f for this transcendental equation can yield approximate results of 4.1 and 9.1 GHz, respectively, which has shown a good agreement with simulated results in Fig. 2(c).

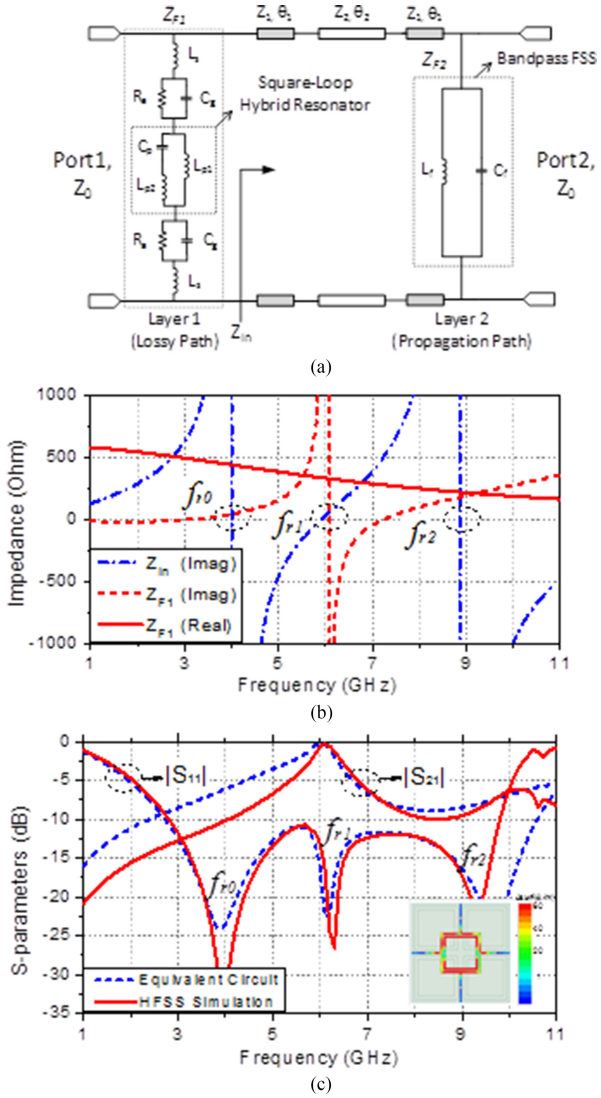

Fig. 2. (a) Equivalent circuit model of the proposed AFST structure under the normal incidence. (b) Input impedance of Z_{in} and impedance of the absorption layer Z_{F1}. (c) Comparison between full-wave simulation and equivalent circuit. (Circuit parameters: $Z_0 = 377\,\Omega$, $Z_1 = 217\,\Omega$, $\theta_1 = 12°$ at 10 GHz, $Z_2 = 377\,\Omega$, $\theta_2 = 132°$ at 10 GHz, $R_a = 294\,\Omega$, $L_s = 4.1$ nH, $L_{p1} = 2.6$ nH, $L_{p2} = 2.4$ nH, $L_f = 5$ nH, $C_g = 0.08$ pF, $C_p = 0.14$ pF, $C_f = 0.16$ pF, Inset: current distribution on SLHR resonator at 6 GHz.)

The first layer of SLHR is utilized to achieve a passband within the absorption band and expand the upper absorption bandwidth. According to the equivalent circuit model in Fig. 2(a), the parallel resonant frequency f_p and series resonance frequency f_s for SLHR are expressed as

$$f_p = \frac{1}{2\pi\sqrt{C_p(L_{p1} + L_{p2})}} \tag{4}$$

$$f_s = \frac{1}{2\pi\sqrt{C_p L_{p2}}} \tag{5}$$

where the value of inductors L_{p1} and L_{p2} is related to the side length of inner and outer loops on the first layer, respectively.

C_p is determined by the gap width g_1 between the two loops. At the parallel resonant frequency of f_p, the lossy path is disconnected, which means that the incident wave can pass through with ideally no loss. In addition, the series resonance frequency at f_s is very close to the upper absorption frequency f_{r2}. Under this situation, the resistors are reconnected at f_s, making the lossy layer effective again. Therefore, the upper absorption bandwidth has been expanded with this resonance.

For the bandpass FSS at the second layer, the cross-shaped frame and the notched gap are equivalent to an inductor L_f and a capacitor C_f in parallel connection. The expression of FSS's passband frequency f_b is

$$f_b = \frac{1}{2\pi\sqrt{C_f L_f}}. \tag{6}$$

According to the transmission conditions derived in [9], both the first and second layers in Fig. 2(a) have to satisfy a parallel resonance at the same frequency f_{r1}. Based on this, we obtain $f_p = f_b = f_{r1}$. To gain insight into the operating principle of the proposed structure, the current distribution on the first layer at 6 GHz is plotted in the inset of Fig. 2(c). It is seen that within the passband, current is mainly distributed on the square loops due to its parallel resonance. As a result, almost no current flows through resistors, which leads to little loss. Due to the geometrical symmetry of these patterns, it is easy to find that the unit cell acts the same for incident waves of all polarizations under the normal incidence.

The simulated *S*-parameter results using ANSYS HFSS simulation tool and equivalent circuit model are compared in Fig. 2(c). The equivalent circuit has well predicted the performance of the proposed structure. It is shown that a passband with 0.29 dB insertion loss at 6.1 GHz can be achieved. The bandwidth with $|S_{11}| < -10$ dB ranges from 2.8 to 9.8 GHz, corresponding to a fractional bandwidth of 112.4%. In addition, the passband with –3 dB insertion loss is from 5.7 to 6.5 GHz, which represents a fractional bandwidth of 13%.

The performance of oblique incidence for this structure is further studied in Fig. 3. The scan plane of oblique incidence angle θ is located in the *yz* plane and *xz* plane, for TE wave and TM wave, respectively. It is shown that the passband and absorption band have a frequency shift at small angles of oblique incidence. This frequency shift under the oblique incidence may be attributed to a different induced inductance and capacitance.

III. Design Example and Experimental Results

In order to verify the design concept presented in Section II, a design example is fabricated and tested. In this design, same material is used for both the first and second layers. The substrate material for fabrication is Rogers 4230, with its dielectric constant of 3 and thickness of 1.016 mm. Fig. 4(a) and (b) shows the photograph of the fabricated prototype, which consists of 1 × 6 unit cells with a size of 24 × 144 mm^2. The unit cell dimensions follow the previous design with a periodic boundary condition. The fabricated sample consists of 24 lumped resisters with a value of 294 Ω (Part No.: ERA-2AEB2940X). It should be pointed out that the number of lumped elements in this unit cell has reduced by four times, compared with the design in [9].

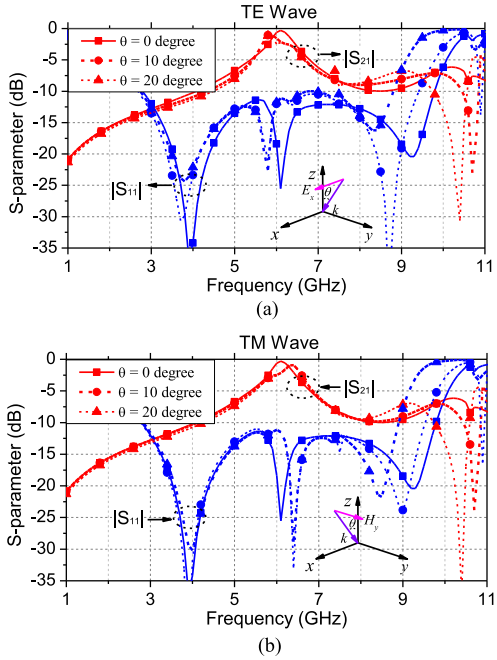

Fig. 3. Simulated reflection coefficient and transmission coefficient of the proposed AFST unit cell under an oblique incidence. (a) TE-polarized wave. (b) TM-polarized wave.

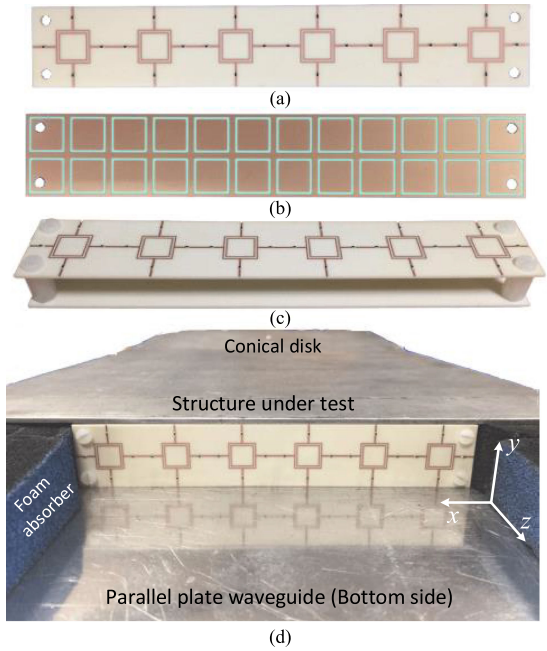

Fig. 4. Assembly details and measurement setup of proposed structure. (a) First layer of AFST. (b) Second layer of AFST. (c) Assembled structure with nylon screws and spacers. (d) Photograph of the measurement setup in a PPW.

A sample of the fabricated AFST is shown in Fig. 4(c). It is then measured in a parallel-plate waveguide (PPW) test setup. The details of this measurement setup can be found in [14]. Fig. 4(d) shows the configuration of AFST in the PPW. It is mentioned that the upper plate of PPW is removed in this figure to have a better view of the test setup. The traveling TEM wave inside the PPW is launched by two conical disks located at the both ends of the test setup. To ensure no reflection from

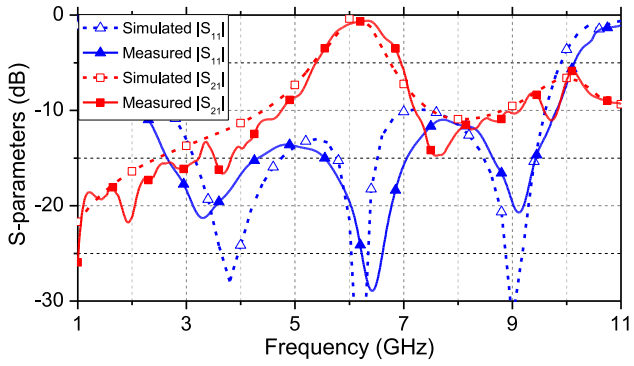

(a)

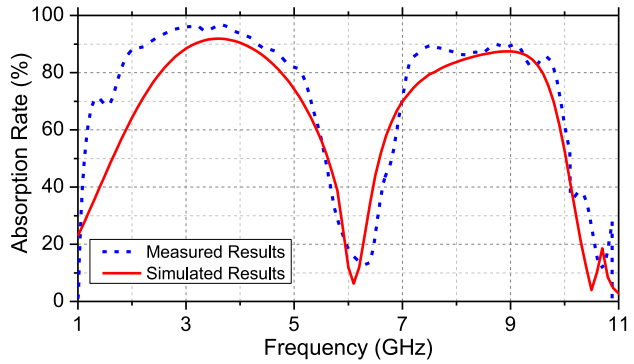

(b)

Fig. 5 (a) Simulated and measured results of $|S_{11}|$ and $|S_{21}|$ for the fabricated AFST under the normal incidence. (b) Comparison of the simulated and measured absorption rate results.

TABLE I
COMPARISON OF THE EXISTING 2-D AFST DESIGN IN THE LITERATURE

Reference	Insertion Loss (dB)	Lower Absorption Bandwidth[2]	Upper Absorption Bandwidth[2]	Thickness (λ_L)	Number of Lumped Elements[3]
[6][1]	0.33	N.A.	71.1%	0.080	N.A.
[7][1]	0.30	N.A.	105.1%	0.103	8
[11][1]	0.20	103.2%	N.A.	0.120	4
[12][1]	0.50	92.8%	N.A.	0.112	4
[9]	0.36	25.1%	11.5%	0.113	18
[10]	0.40	61.1%	37.7%	0.124	16
[13]	0.36	41.3%	20.7%	0.110	8
This work	0.29	91.4%	31.9%	0.104	4

[1]These designs have only one-sided absorption band.
[2]The bandwidths are for 80% absorption rate.
[3]Number of lumped components required in a unit cell.

two side walls, they are covered with foam absorbers. It should be mentioned that the test frequency range of this waveguide setup covers the operating frequency range of our AFST to be measured.

Fig. 5 shows the comparison of simulated and measured transmission and reflection coefficients of the proposed AFST structure under the normal incidence. It is clear that simulated and measured results are in a good agreement. The small difference between these results is attributed to the errors of fabrication and measurement. In addition, the measured results indicate a transmission window with 0.6 dB insertion loss at 6.3 GHz. The fractional bandwidth for this passband with less than 3 dB insertion loss is 21.3%. It is shown that the reflection coefficient is below –10 dB from 2.1 to 9.8 GHz, corresponding to a fractional bandwidth of 129.1%. It is expected that the structure has more than 80% absorption for an incident wave from 1.9 to 5.1 GHz and from 7.1 to 9.8 GHz, which represents a bandwidth of 91.4% and 31.9%, respectively. It is seen that the measured absorption bandwidth is larger than the simulated one and the reason for this difference is because of the parasitic effect of lumped resistors. Apparently, this parasitic effect is not taken into consideration in the full-wave simulations, for the sake of a simplified model. The comparisons between our design of AFST and others in the literature are listed in Table I.

IV. CONCLUSION

It has been shown that a transmission window within a wide absorption band can be introduced by employing square-loop hybrid resonator in a unit cell. The parallel and series resonances of the SLHR are both utilized in this case. Detailed analysis and an equivalent circuit model for this structure have been presented. Measured results agree well with the simulated ones. A comparison between other AFST designs based on 2-D unit cell in the literature has been performed, and it shows that our proposed AFST has the widest bandwidth for –10 dB reflection coefficient and the least amount of lumped elements required in a unit cell. The potential application for the proposed structure is to achieve an out-of-band RCS reduction when integrated with an antenna.

REFERENCES

[1] B. A. Munk, *Frequency Selective Surfaces: Theory and Design*. New York, NY, USA: Wiley, 2000.
[2] A. A. Omar, Z. Shen, and H. Huang, "Absorptive frequency-selective reflection and transmission structures," *IEEE Trans. Antennas Propag.*, vol. 65, no. 11, pp. 6173–6178, Nov. 2017.
[3] B. Li and Z. Shen, "Wideband 3D frequency selective rasorber," *IEEE Trans. Antennas Propag.*, vol. 62, no. 12, pp. 6536–6541, Dec. 2014.
[4] Z. Shen, J. Wang, and B. Li, "3-D frequency selective rasorber: Concept, analysis, and design," *IEEE Trans. Microw. Theory Techn.*, vol. 64, no. 10, pp. 3087–3096, Oct. 2016.
[5] Y. Yu, Z. Shen, T. Deng, and G. Luo, "3-D frequency-selective rasorber with wide upper absorption band," *IEEE Trans. Antennas Propag.*, vol. 65, no. 8, pp. 4363–4367, Aug. 2017.
[6] F. Costa and A. Monorchio, "A frequency selective radome with wideband absorbing properties," *IEEE Trans. Antennas Propag.*, vol. 60, no. 6, pp. 2740–2747, Jun. 2012.
[7] Q. Chen, J. Bai, L. Chen, and Y. Fu, "A miniaturized absorptive frequency selective surface," *IEEE Antennas Wireless Propag. Lett.*, vol. 14, pp. 80–83, 2015.
[8] B. Yi, L. Yang, and P. Liu, "Design of miniaturized and ultrathin absorptive/transmissive radome based on interdigital square loops," *Prog. Electromagn. Res. Lett.*, vol. 62, pp. 117–123, 2016.
[9] Y. Shang, Z. Shen, and S. Xiao, "Frequency-selective rasorber based on square-loop and cross-dipole arrays," *IEEE Trans. Antennas Propag.*, vol. 62, no. 11, pp. 5581–5589, Nov. 2014.
[10] K. Zhang, W. Jiang, and S. Gong, "Design bandpass frequency selective surface absorber using LC resonators," *IEEE Antennas Wireless Propag. Lett.*, vol. 16, pp. 2586–2589, 2017.
[11] Q. Chen, S. Yang, J. Bai, and Y. Fu, "Design of absorptive/transmissive frequency-selective surface based on parallel resonance," *IEEE Trans. Antennas Propag.*, vol. 65, no. 9, pp. 4897–4902, Sep. 2017.
[12] Q. Chen, L. Chen, J. Bai, and Y. Fu, "Design of absorptive frequency selective surface with good transmission at high frequency," *Electron. Lett.*, vol. 51, no. 12, pp. 885–886, Jun. 2015.
[13] X. Xiu, Y. Han, W. Che, and W. Yang, "Double-polarization frequency selective rasorber based on cross-frame and circle ring slot arrays," *Proc. 10th Global Symp. Millimeter-Waves*, Hong Kong, 2017, pp. 109–111.
[14] Y. Shang, Z. Shen, and S. Xiao, "On the design of single-layer circuit analog absorber using double-square-loop array," *IEEE Trans. Antennas Propag.*, vol. 61, no. 12, pp. 6022–6029, Dec. 2013.